Regenerative Biomaterials, 2016, 33–40
doi: 10.1093/rb/rbv025
Advance Access Publication Date: 31 December 2015
Research Article

OXFORD

Comparison of bone regeneration in alveolar bone of dogs on mineralized collagen grafts with two composition ratios of nano-hydroxyapatite and collagen

Yan-Fu Wang[1], Cheng-Yue Wang[2,*], Peng Wan[3], Shao-Gang Wang[3] and Xiu-Mei Wang[4]

[1]Graduate School, Liaoning Medical University, Jinzhou 121000, China; [2]Department of Prosthodontics, Affiliated Stomatological Hospital of Liaoning Medical University, Jinzhou 121000, China; [3]Shenyang National Laboratory for Materials Science, Institute of Metal Research, Chinese Academy of Sciences, Shenyang 110016, China; [4]Institute for Regenerative Medicine and Biomimetic Materials, School of Materials Science and Engineering, Tsinghua University, Beijing 100084, China

*Correspondence address. Department of Prosthodontics, Affiliated Stomatological Hospital of Liaoning Medical University, Jinzhou 121000, China. Tel: +86-416-2322071; Fax: +86-416-2332215; E-mail: wchy1758@sohu.com

Received 3 September 2015; revised 11 November 2015; accepted 12 November 2015

Abstract

To study the effect of two composition ratios of nano-hydroxyapatite and collagen (NHAC) composites on repairing alveolar bone defect of dogs. Eighteen healthy adult dogs were randomly divided into three groups. Two kinds of the NHAC composites were prepared according to the constituent ratios of 3:7 and 5:5; immediately after extraction of the mandibular second premolars, each kind of the NHAC composite was implanted into extraction socket, respectively: Group I, nHA/Col = 3:7; Group II, nHA/Col = 5:5 and Group III, blank control group. The bone-repairing ability of the two grafts was separately analyzed by morphometric measurement, X-ray tomography examination and biomechanical analysis at 1st, 3rd and 6th month post-surgical, respectively.
The NHAC composites were absorbed gradually after implanting into alveolar bone defect and were replaced by new bone. The ratios of new bone formation of Group I was significantly higher than that of Group II after 3 months ($P < 0.05$). The structure and bioactive performance can be improved when the ratio between the collagen and the hydroxyapatite was reasonable, and the repairing ability and effect in extraction sockets are obviously better.

Keywords: nano-hydroxyapatite; collagen; dental extraction socket; alveolar ridge preservation; ratios

Introduction

It is well accepted by the scientific community that the physiological dimensional changes occur on the alveolar ridge after tooth extraction which is one of the most widely performed dental procedures [1–5] and the resorption reaches a mean horizontal reduction of 3.79 mm and mean vertical reduction of 1.24 mm at 6th month [6]. These height (corono-apical) and width (bucco-lingual) alterations in the alveolar bone cannot be prevented by implants placing immediately into the extraction sockets but reduce the level of the resorption [3, 7].

Bone graft materials are utilized to augment or maintain the space for bone regeneration. Various implant options are available to solve the issue of bone defects, and all the techniques have advantages and disadvantages [8–11]. Currently, the number of bone substitutes that have all the characteristics and properties of autologous bone such as osteogenesis, osteoconduction and osteoinduction, with no inflammatory response and mechanical competence is zero [12]. Synthetic calcium phosphate ceramic materials, for instance hydroxyapatite (HA), are widely used as bone grafts due to their similarity in the chemical composition of bone mineral matrix, resulting in superior biocompatibility, osteoconductivity and osteointegration properties, and the *in vitro* evaluation of HA showed the reduction of osteoclast and the increase in osteoblastic activity characterized by doubling in synthesis of alkaline phosphatase, osteocalcin and collagen (Col) type I [13]. Additionally, Col has many advantages as a naturally derived biomaterial. It shows excellent biocompatibility, biodegradability and interconnected porous architecture but possesses poor load bearing capability [14]. Both HA and Col had earned merit for bone regeneration as the enhanced of the bioactivity of the scaffold by providing a source of calcium and phosphate ions that could be used by osteogenic cells to create new bone.

In this study, we developed different composition ratios of nano-hydroxyapatite and collagen (NHAC) composites that have some features of natural bone in both composition and microstructure. These materials are the two major constituents of bone and a logical choice as the basis of a biomimetic scaffold capable of supporting and promoting bone regeneration [15]. The first aim of this work was to test the efficacy of these systems in reducing the resorption of the alveolar bone. The second aim was to compare the level of early bone formation. The third aim was to acquire a deeper understanding of HA–Col scaffold interactions, ultimately leading to optimal scaffold design and contributing to the goal of safe and efficient therapies in the clinical.

Materials and methods

Study animals and ethics

Eighteen healthy male beagle dogs (each ~15 kg and a mean age of 18 months) were included in the experiment and randomly divided into three groups (Groups A, B and C). All the research protocols were approved by the ethical committee of Liaoning Medical University (Jinzhou, China).

Bone graft materials

The NHAC composites were provided by Allgens Co. Ltd. (Beijing, China). The composite was prepared as described in previous publications [16, 17]. The parameters of the composites are listed in Table 1. The theoretical constituent ratios of the NHAC composites were determined by residue on ignition. And the X-ray photoelectron spectroscopy was performed with a Thermo ESCALAB 250 (VG Scientific Co., UK) using monochromatic Al Ka radiation (1361.1 eV) as the excitation source. All spectra were acquired at a pass energy of 20 eV with the anode operated at 150W. The results were shown in Fig. 1.

Table 1. The percentage of each component in weight and the parameters of the composites

Property	NHAC 1	NHAC 2
HA/Col in weight	3:7	5:5
Porosity (%)	85-95	85-95
Diameter of pore (μm)	50-500	50-500

Surgical protocol and animal subgroups

All surgical procedures were performed under general anesthesia by intramuscular injecting xylazine hydrochloride injection (0.1 mg/kg, Huamu Corp., Changchun, China). After disinfection of the surgical site with 1% providone-iodine solution, local anesthesia was provided (Articaine HCl 2% with epinephrine 1:100 000, Acteon Corp., Bordeaux, France) at the respective buccal and lingual sites by infiltration. The second premolars in both quadrants of the mandible were removed. Minimal displacement of the tissue was performed to expose the buccal and lingual alveolar bony plates. The bucco-lingual full thickness flaps were elevated. Both the mesial and distal roots of the sockets were used for implant placement. The sockets were irrigated with normal saline, dried with sterile gauze and filled carefully with the various graft materials to the marginal bony crest as Fig. 2 and we had:

Group I—HA: Col = 3:7 (12 sites)
Group II—HA: Col = 5:5 (12 sites)
Group III—control (no filling, 12 sites)

Postoperative management

The soft tissue of the extraction site was coronally advanced and sutured closely. The CT scans were made for each animal (SOMATOM Spirit, SIEMENS, German) to measure the vertical distance around region of interest (ROI) immediately after the surgery. Post-surgical care including intramuscular administration of cefazoline sodium (North China Pharmaceutical Corp., Shijiazhuang, China) and daily topical dressing with 0.2% chlorhexidine solution (Retouch Corp., Dezhou, China) was applied. Daily inspections of the wounds for clinical signs of complications were also performed. All animals were placed on a soft diet for 10 days. The sutures were removed after 7 days.

Sacrifice

Two animals from each group were euthanized, respectively, at 1, 3 and 6 months after the surgery applying an overdose of sodium

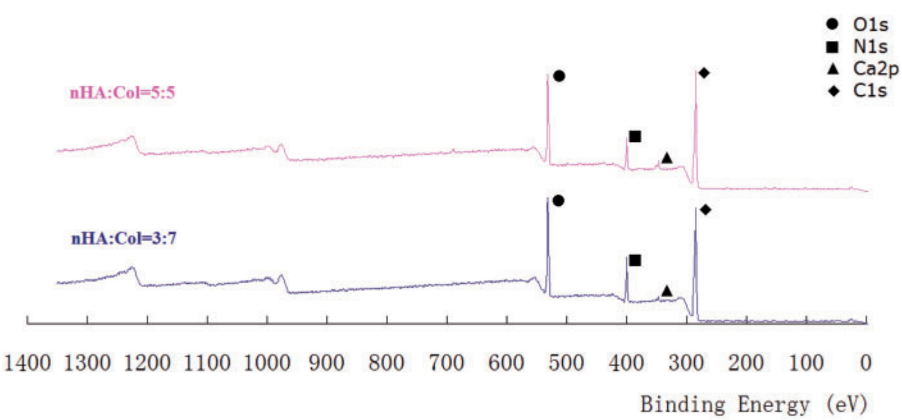

Figure 1. Comparison between the two NHAC composites with X-ray photoelectron spectroscopy spectra

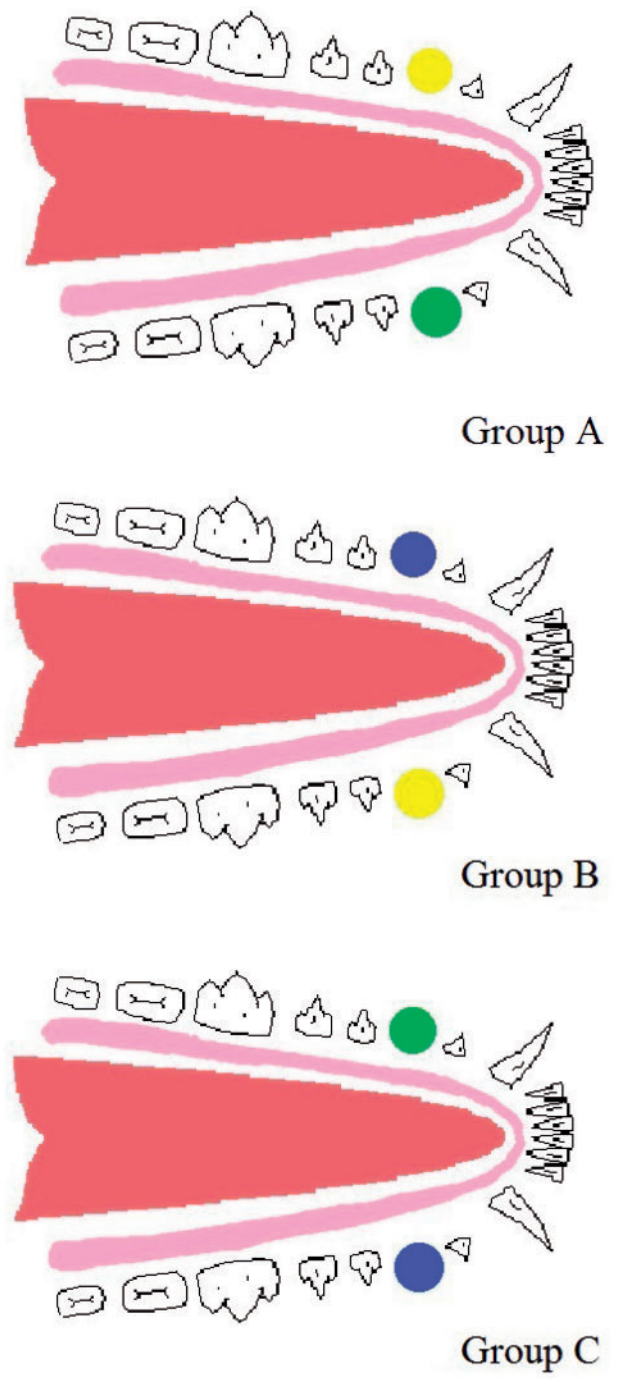

Figure 2. Study design for Group I (yellow), Group II (green) and Group III (blue)

thiopental and perfused with a fixative containing the mixture of 5% glutaraldehyde and 4% of formaldehyde.

Bone tissue morphometric measurement

The vertical distance around the ROI of the alveolar bone was measured from the upper to the lower edge of the mandible to determine the resorption rate of hard tissue using slide caliper (GPI Co. LTD., Shanghai, China).

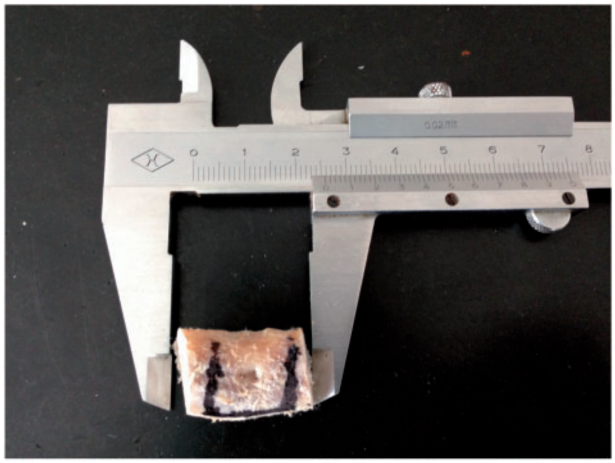

Figure 3. The alveolar bone around the extraction socket was cutting into a bone block that the size of it was approximately 25 mm × 15 mm × 10 mm. The black line represents the scan area

Radiographic examination

High resolution X-ray tomography tests were performed on a 3D X-ray microscope (XRM, Xradia Versa XRM-500, Zeiss Corp., Oberkochen, Germany) to evaluate the newly formed bone. The typical size of the bone specimen demonstrated in Fig. 3 was approximately 25 mm × 15 mm × 10 mm. The scanning voltage was 80 kV, and the exposure time was 1s. A total of 1600 projections were acquired while the specimen was rotated about 360°. The pixel size was 22.4814 μm. Then, the visualization and quantification of the newly formed bone were fulfilled on Avizo Fire (Visualization Sciences Group, FEI Corp., OR) image analysis software. The newly formed bone and buccal and lingual bone plate were displayed in different colors. The trabecular bone volume percentage and the bone porosity (BP) were also given.

Biomechanical analysis

Compression strength testing was carried out at 3 months post-surgical using a MTS testing machine (CMT 4304, MTS Systems Corp., MN). The rectangular bone blocks used in the compression tests were grinded into accurately 18 mm × 7 mm ×12 mm. The specimen was placed on a specially designed platform with a self-aligning function to ensure vertical compress. A pre-load of 40N with 30s of accommodation time followed by continuous and progressive load at a speed of 0.1 mm/min was applied. The first peak force (judged as the yield load in the force-displacement diagram) detected during the test was recorded as the ultimate strength.

Statistical analysis

The results were reported as the mean and the standard deviation (mean ± SD). All statistical analyses were performed on a personal computer using SPSS, version 13.0 (IBM, Somers, NY). An alpha level of 0.05 was set as the desired significance level. Two-way analysis of variance was employed to assess the effects of two independent variables (bone graft and time period) and one-way analysis of variance was used to determine the effect of one independent variable (bone graft). When such interaction was significant, Student's *t*-test was performed to compare the effect in bone repairing between experimental proportions of each bone substitute.

RESULTS

Clinical observations

Healing was uneventful at all sites with no clinical signs of aberrant inflammation or other complications throughout the entire experimental period. All experimental sites were fully closed with the gingival epithelium though the regions of the extraction socket was depressed compared with the other tissue after two weeks.

Morphometric measurement

Immediately after the surgery, the vertical distance of the alveolar bone was 18.67 ± 0.62 mm, 18.72 ± 0.75 mm and 18.39 ± 0.65 mm for Group I, Group II and Group III, respectively. At 1 month post-surgical, the height of mandible (corono-apical) in Group I was 16.84 ± 0.36 mm, the height in Group II was 16.68 ± 0.40 mm and in Group III was 15.95 ± 0.43 mm. No statistical differences were found among three groups ($P > 0.05$). However, after 3 months, the height of alveolar bone exhibited for Group I (15.76 ± 0.28 mm), Group II (14.88 ± 0.36 mm) and Group III (13.77 ± 0.34 mm) which was decreased prominently. And after 6 months, the dimensions change into 14.83 ± 0.27 mm for Group I, 13.82 ± 0.36 mm for Group II and 12.36 ± 0.32 mm for Group III. The resorption of the ROI was increased ($P < 0.01$) in comparison with that at 1 and 3 month postoperative (Fig. 4B). In addition, we observed a significant difference among the three groups ($P < 0.01$) after 3 months. The hard tissue in Group I was the highest among all groups, whereas the severe resorption of alveolar bone occurred in Group III (Fig. 4A). And after 6 months, Group I resisted to the bone resorption and the minimal alveolar bone loss compared with 1 and 3 month postoperative.

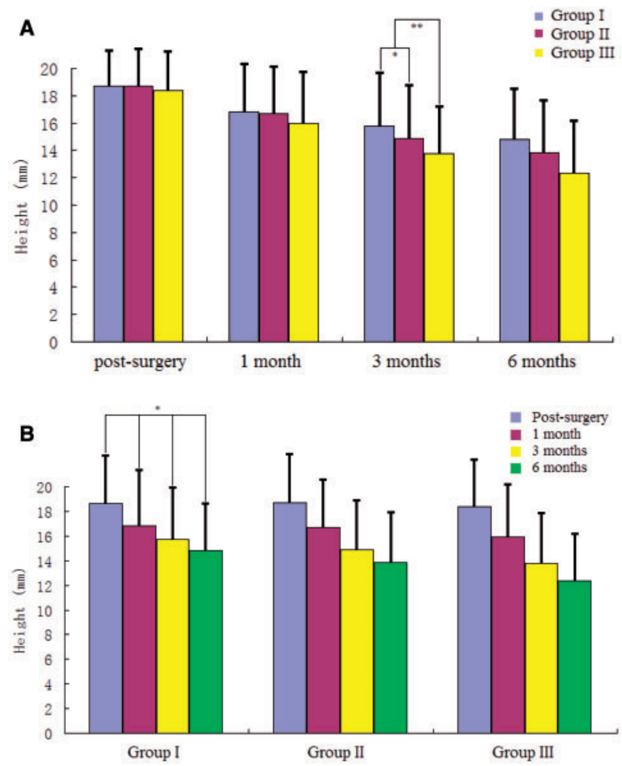

Figure 4. The dimensional changes of mandible of each group in different time periods. (**A**) Result of morphometric measurement among three groups in different time periods. *$P < 0.01$; **$P < 0.01$. (**B**) Result of morphometric measurement in different tine periods among three groups. *$P < 0.01$

XRM analysis

At first month after the surgery, we observed remarkable hard tissue alterations and the bone defect was clearly visible. The area of extraction socket was filled mainly by woven bone (immature) and a small amount of lamellar bone (mature) and the NHAC material was barely present in Group I and Group II (Fig. 5A and B). In Group III, the woven bone was recognized (Fig. 5C).

At third month, the bone defect was still evident. In Group I and Group II, the graft material could not be identified, and the lamellar and woven bone was observed (Fig. 5D and E), although the bone defect was not completely closed. In Group III, woven bone, and, to a lesser extent, lamellar bone were observed (Fig. 5F).

At 6th month, in Group III, the defect areas were still visible. They were composed of woven bone, and the mature bone was also detected at the periphery of the cavity (Fig. 5I). The bone defect could hardly be detected in Group I and Group II (Fig. 5G and H).

The trabecular bone volume percentage and BP in different time periods are listed in Tables 2 and 3.

Biomechanical analysis

The average lengths of all bone blocks were, respectively, 18.7 ± 1.2 mm, 17.4 ± 1.0 mm and 17.9 ± 1.4 mm in Group I, Group II and Group III. The average widths of all bone blocks were, respectively, 6.8 ± 0.8 mm, 7.6 ± 0.5 mm and 6.9 ± 1.0 mm in Group I, Group II and Group III. The average heights of all bone blocks were, respectively, 12.7 ± 0.6 mm, 11.4 ± 1.0 mm and 11.9 ± 0.7 mm in Group I, Group II and Group III. The mean compressive forces were 3511.3 ± 148.6N for Group I, 3930.3 ± 92.1N for Group II and 3346.6 ± 174.3N for Group III. The mean displacements of failure compressive strength were 0.56 ± 0.01 mm for Group I, 0.62 ± 0.02 mm for Group II and 0.54 ± 0.01 mm for Group III. The results of three groups are listed in Table 4.

Discussion

To solve the problems associated with existing treatment regimen, researchers were trying to develop polymers, ceramics, metals, etc. [7, 11, 18–21]. Any material considered for use as a bone substitute must meet the following requirements: (i) it must be fully biocompatible, (ii) it must be able to serve as an anchoring surface for host cells, (iii) it must have a porosity that allows osteoconduction and (iv) it must be progressively resorbed and replaced by new bone (creeping-substitution) [10]. The materials used in this study were basically satisfying the above requirements.

The bone is a typical complex tissue with hierarchical structure that consists of approximately 70% of HA and 30% of Col by weight and water is the third elementary component (with the dissolved non-collagenous organic matter) [22]. HA, as the main inorganic salt of bone, is the most studied calcium phosphate material ever since 1970s [23, 24]. The clinical use of HA materials, due to they are excellent carriers of osteoinductive growth factors and osteogenic cell populations, are mainly in the form of granules or blocks, depending on the bone defect to be filled. The solubility, biological and mechanical properties of HA materials depend on the crystal size, the ionic impurities, the specific surface area and the porosity [25, 26]. Unfortunately, the HA material is resorbed slowly and the large segments of it could remain in place for years. Furthermore, the Col protein is the major organic matter of the bone (predominantly type I) and it provides strength and toughness to the bone

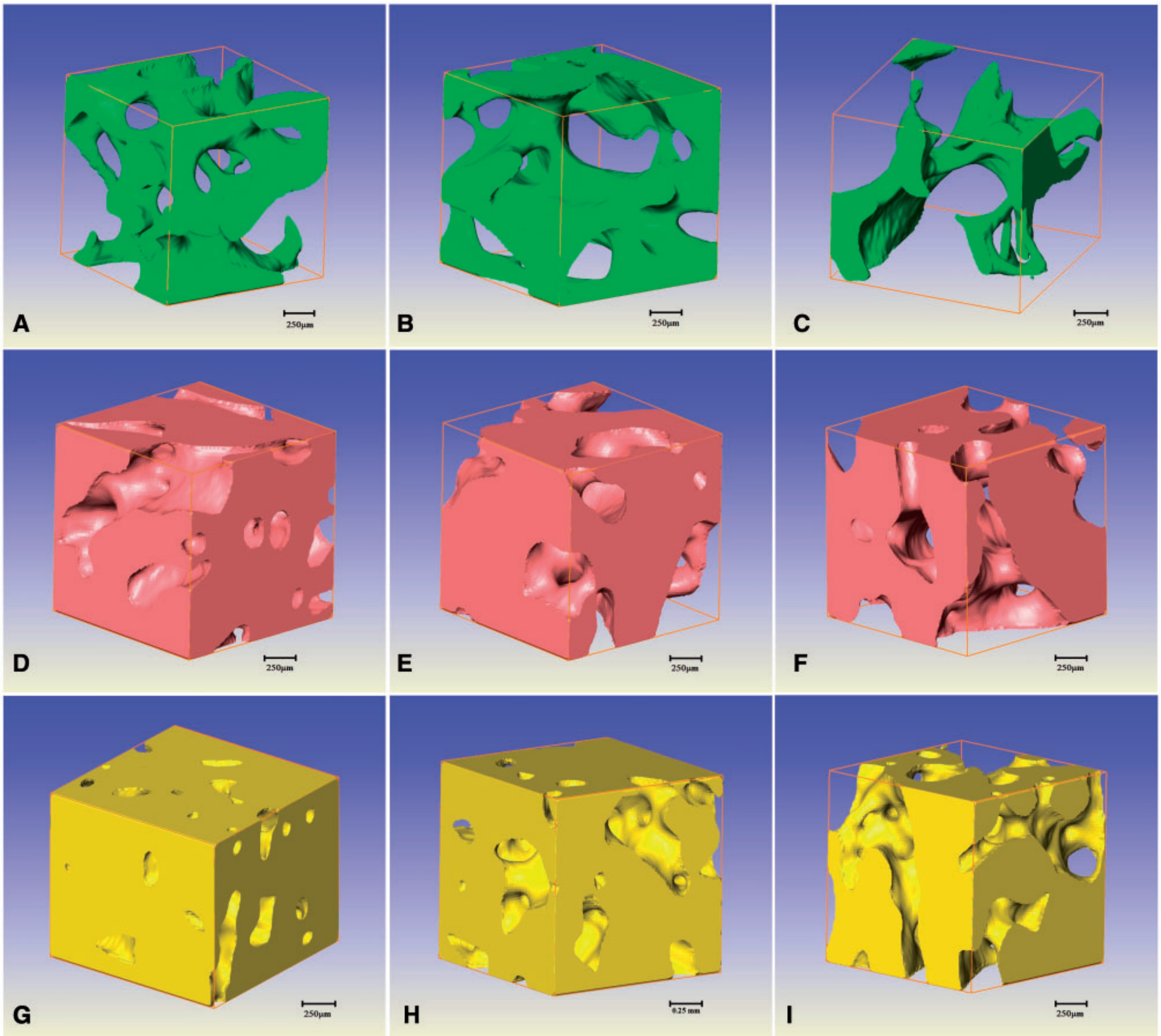

Figure 5. The details of the specimens in the XRM examination at 1, 3 and 6 months. The specimens in different time periods were shown in different colors. (**A**) The specimen of Group I after 1 month. The area of extraction socket was filled by immature bone. The array of it was messy. (**B**) The specimen of Group II after 1 month. (**C**) The specimen of Group III after 1 month. The area of extraction socket was filled mainly by woven bone. (**D**) The specimen of Group I after 3 months. The newly formed bone had become compact. (**E**) The specimen of Group II after 3 months. (**F**) The specimen of Group III after 3 months. The mature bone had become more while the woven bone was still recognized. (**G**) The specimen of Group I after 6 months. The extraction socket was filled by mature bone. (**H**) The specimen of Group II after 6 months. (**I**) The specimen of Group III after 6 months. The woven bone and the mature bone were visible

Table 2. The trabecular bone volume percentage of each group in different time periods (%)

Group	1 Month	3 Months	6 Months
I	14.43 ± 0.77	22.22 ± 0.43	53.43 ± 0.57
II	14.27 ± 0.96	20.25 ± 0.36	50.60 ± 0.82
III	8.33 ± 0.98	17.35 ± 0.55	42.75 ± 0.44

There was no statistical difference between Group I and Group II ($P > 0.05$), whereas both of them were greater than Group III ($P < 0.01$) at 1month. The trabecular bone volume percentage of all groups had increased ($P < 0.01$). And there was a significant difference among all three groups after 3 months ($P < 0.01$).

Table 3. The BP of each group in different time periods (%)

Group	1 Month	3 Months	6 Months
I	55.23 ± 0.68	23.59 ± 0.83	15.22 ± 0.98
II	55.01 ± 0.73	27.61 ± 0.61	19.01 ± 0.72
III	56.27 ± 0.70	39.38 ± 0.71	26.11 ± 0.77

There was no statistical difference among three groups at 1 month ($P > 0.05$). The BP had decreased during the experimental period ($P < 0.01$). And there was a significant difference among all three groups after 3 months ($P < 0.01$).

Table 4. The ultimate strength of each group in different time periods (MPa)

Group	No. 1	No. 2	No. 3	No. 4	Mean	Standard deviation	*F*	*P*
I	25.16	25.33	24.51	25.41	25.1025	0.41	160.5393	<0.01
II	30.14	29.81	31.26	30.79	30.50	0.65		
III	23.09	22.79	23.64	21.84	22.84	0.75		

[15, 27, 28]. As Col is easily degraded and resorbed, and its mechanical properties are relatively low, we have developed different composition ratios of HA-Col composites that are highly porous and easily remodeled by cells to make it efficient in repairing hard tissue defects.

In this study, the dimensional alterations of alveolar ridge with using the NHAC materials in extraction sockets were significant less than that without using the materials after 3 months and the height of mandible in Group I was higher than that in Group II. Despite the fact that the present experiment clearly demonstrated that the implantation of the NHAC materials did not prevent the resorption of the alveolar ridge, the benefit of materials to the newly formed bone is obviously and there is a significant difference in the effect between the two ratios of the materials. This discrepancy could be partially explained by the properties of enhance osteoblast differentiation [29]. In this study, we chose the XRM examination because this technique has many advantages including high spatial resolution, multiscale imaging, non-destructive three-dimensional visualization and quantification [32–34]. The structure of the NHAC scaffold is an interspersed composite of HA nanoparticles and Col fibers [35], and the Col component is arranged in a triple-helical conformation. The calcium ions promote the adhesion of bone cells and stimulate its subsequent activity, and the composites show the high percentage on the alkaline phosphatase activity [30, 31]. And the scaffolds have a more reasonable degradation rate. The results of XRM analyses (Figs 6 and 7) are in agreement with those from other report on experimental studies on implants placed into extraction sockets in dogs that have shown a limited improvement in bony crest preservation compared to untreated sites [36]. They indicated the high osteoconductivity and bioactivity of the NHAC materials and the material with more HA would decrease the quantity of the new formed bone. The Col fiber provided the path for the osteoblast cells to creep into the materials and then replace them. However, the non-absorbable of HA would reduce the effect of replacement for osteoblast cells. To overcome the limitations of HA, a more efficient strategy would be to reduce the content of HA, which, if properly chosen, would assist with both the HA and the Col to the integration with the surrounding tissue [37].

One noteworthy observation was that the ultimate strength of the specimens with the NHAC material was significant stronger than those without materials. Composites behaved mechanically in a superior way to the individual components. Although the quality of cortical and trabecular bone can be classified according to the elastic properties which depend on the bone density and the relative bone density [38, 39], the results of the present experiment indicated that the maximal strength of the alveolar bone with the NHAC materials was associated to the component proportion and property of the materials. The ductile properties of Col help to increase the poor fracture toughness of HA, and the addition of calcium phosphate compound gave higher stability and load bearing capability to the Col [18, 40]. In addition, a confounding factor cannot be ignored is

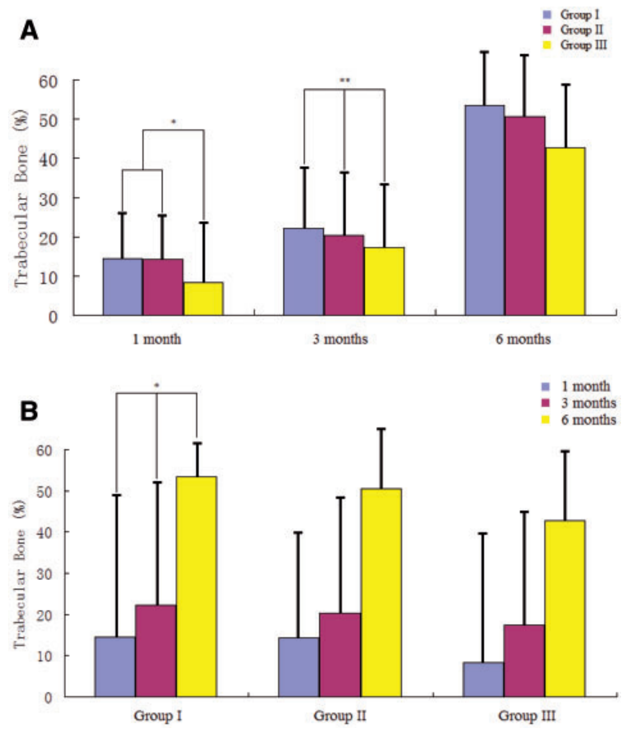

Figure 6. The trabecular bone volume percentage of each group in different time periods. (**A**) The trabecular bone volume percentage among three groups in different time periods. $*P<0.01$; $**P<0.01$. (**B**) The trabecular bone volume percentage in different tine periods among three groups. $*P<0.01$

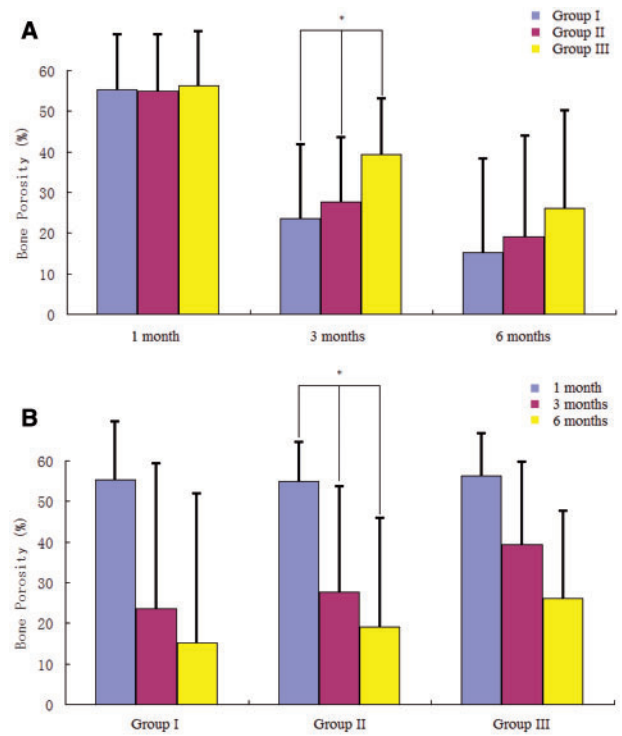

Figure 7. The BP of each group in different time periods. (**A**) The BP among three groups in different time periods. $*P<0.01$. (**B**) The BP in different time periods among three groups. $*P<0.01$

that the compressive strength of normal mandible bone around the ROI. Therefore, we tried to grind the bone blocks into the size exactly. And the individual differences in morphology or geometry can be problematic in cadaveric experiments [41], the affects about the size and geometry of the bone blocks in the compressive test should be investigated in future studies.

Conclusion

This study demonstrated the effect on biological and mechanical properties of the NHAC materials and compared the effects among different ratios in repairing the extraction socket. The ratios in weight of each component are important. The NHAC composite with a Col-more proportion could express the potential of fast bone tissue formation; in contrast, the mechanical property could be relatively poor and vice versa. An ideal composition ratio for the NHAC composite material could reduce the influence of physiological dimensional changes occurred on the alveolar ridge.

Acknowledgements

The authors would like to acknowledge Mr Yi-Bin Ren for his assistance with biomechanical analysis and Mr Tian-Xi Song, Mr Yu-Sheng Yao, Mr Lu-Ming Tian, Mr Yuan Zhao, Mr Yi Sun and Ms. Man Yang for their helpful discussions. The authors also wish to express their gratitude to Mr Fu-Zhai Cui for his careful reading of the manuscript.

Funding

This work was supported by the National Natural Science Foundation of China (grant no. 21371106) and the Science & Technology Project of Liaoning Province (grant no. 2015020689).

Conflict of interest statement. None declared.

References

1. Pietrokovski J, Massler M. Alveolar ridge resorption following tooth extraction. *J Prosthet Dent* 1967;**17**:21–7.
2. Darby I, Chen S, De Poi R. Ridge preservation: what is it and when should it be considered. *Aust Dent J* 2008;**53**:11–21.
3. Wang RE, Lang NP. Ridge preservation after tooth extraction. *Clin Oral Implants Res* 2012;**23**:147–56.
4. Chappuis V, Engel O, Reyes M *et al*. Ridge alteration post-extraction in the esthetic zone: a 3D analysis with CBCT. *J Dent Res* 2013;**92**:195S–201S.
5. Avila-Ortiz G, Elangovan S, Kramer KWO *et al*. Effect of alveolar ridge preservation after tooth extraction: a systematic review and meta-analysis. *J Dent Res* 2014;**93**:950–8.
6. Tan WL, Wong TL, Wong MC *et al*. A systematic review of post-extractional alveolar hard and soft tissue dimensional changes in humans. *Clin Oral Implants Res* 2012;**23**:157–61.
7. Hong JY, Lee JS, Pang EK *et al*. Impact of different synthetic bone fillers on healing of extraction sockets: an experimental study in dogs. *Clin Oral Implants Res* 2014;**25**:e30–7.
8. Kim YK, Yun PY, Um IW *et al*. Alveolar ridge preservation of an extraction socket using autogenous tooth bone graft material for implant site development: prospective case series. *J Adv Prosthodont* 2014;**6**:521–7.
9. Li WM, Fan JZ, Chen F *et al*. Construction of adipose scaffold for bone repair with gene engineering bone cells. *Exp Biol Med* 2013;**238**:1350–4.
10. Athanasiou VT, Papachristou DJ, Panagopoulos A *et al*. Histological comparison of autograft, allograft-DBM, xenograft, and synthetic graft in a trabecular bone defect: an experimental study in rabbits. *Med Sci Monit* 2010;**16**:BR24–31.
11. Traini T, Piattelli A, Caputi S *et al*. Regeneration of human bone using different bone substitute biomaterials. *Clin Implant Dent Relat Res* 2015;**17**:150–62.
12. Zimmermann G, Moghaddam A. Allograft bone matrix versus synthetic bone graft substitutes. *Injury* 2011;**42**:S16–21.
13. Boanini E, Torricelli P, Gazzano M *et al*. Alendronate-hydroxyapatite nanocomposites and their interaction with osteoclasts and osteoblast-like cells. *Biomaterials* 2008;**29**:790–6.
14. Murphy CM, Schindeler A, Gleeson JP *et al*. A collagen-hydroxyapatite scaffold allows for binding and co-delivery of recombinant bone morphogenetic proteins and bisphosphonates. *Acta Biomater* 2014;**10**:2250–8.
15. Wahi DA, Czernuszka JT. Collagen-hydroxyapatite composites for hard tissue repair. *Eur Cell Mater* 2006;**11**:43–56.
16. Wang RZ, Cui FZ, Lu HB *et al*. Synthesis of nanophase hydroxyapatite/collagen composite. *J Mater Sci Lett* 1995;**14**:490–2.
17. Cui FZ, Du C, Su XW *et al*. Biodegradation of a nano-hydroxyapatite/collagen composite by peritoneal monocyte-macrophages. *Cell Mater* 1996;**6**:31–44.
18. de Val JEMS, Mazon P, Guirado JLC *et al*. Comparison of three hydroxyapatite/β-tricalcium phosphate/collagen ceramic scaffolds: an in vivo study. *J Biomed Mater Res A* 2014;**102**:1037–46.
19. Schneider D, Schmidlin PR, Philipp A *et al*. Labial soft tissue volume evaluation of different techniques for ridge preservation after tooth extraction: a randomized controlled clinical trial. *J Clin Periodontol* 2014;**41**:612–7.
20. Delgado-Ruiz RA, Calvo-Guirado JL, Abboud M *et al*. Porous titanium granules in critical size defects of rabbit tibia with or without membranes. *Int J Oral Sci* 2014;**6**:105–10.
21. Grigolato R, Pizzi N, Brotto MC *et al*. Magnesium-enriched hydroxyapatite as bone filler in an ameloblastoma mandibular defect. *Int J Clin Exp Med* 2015;**8**:281–8.
22. Venkatesan J, Bhatnagar I, Manivasagan P *et al*. Alginate composites for bone tissue engineering: a review. *Int J Biol Macromol* 2014;**72C**:269–81.
23. Hulbert SF, Young FA, Mathews RS *et al*. Potential of ceramic materials as permanently implantable skeletal prostheses. *J Biomed Mater Res* 1970;**4**:433–56.
24. Roy DM, Linnehan SK. Hydroxyapatite formed from coral skeletal carbonate by hydrothermal exchange. *Nature* 1974;**247**:220–2.
25. Verron E, Khairoun I, Guicheux J *et al*. Calcium phosphate biomaterials as bone drug delivery systems: a review. *Drug Discov Today* 2010;**15**:547–52.
26. Dutta SR, Passi D, Singh P *et al*. Ceramic and non-ceramic hydroxyapatite as a bone graft material: a brief review. *Ir J Med Sci* 2015;**184**:101–6.
27. Lee S. Mineralization of type I collagen. *Biophys J* 2003;**85**:204–7.
28. Nair AK, Gautieri A, Chang SW *et al*. Molecular mechanics of mineralized collagen fibrils in bone. *Nat Commun* 2013;**4**:1724
29. Xie J, Baumann MJ, McCabe LR. Osteoblasts respond to hydroxyapatite surfaces with immediate changes in gene expression. *J Biomed Mater Res A* 2004;**71**:108–17.
30. Ribeiro N, Sousa SR, van Blitterswijk CA *et al*. A biocomposite of collagen nanofibers and nanohydroxyapatite for bone regeneration. *Biofabrication* 2014;**6**:035015
31. Zhang SM, Cui FZ, Liao SS *et al*. Synthesis and biocompatibility of porous nano-hydroxyapatite/collagen/alginate composite. *J Mater Sci Mater Med* 2003;**14**:641–5.
32. Wang S G, Wang S C, Lei Z. Application of high resolution transmission X-ray tomography in material science. *Acta Metallurgica Sin* 2013;**49**:897–910.
33. Spath A, Scholl S, Riess C *et al*. STXM goes 3D: digital reconstruction of focal stacks as novel approach towards confocal soft x-ray microscopy. *Ultramicroscopy* 2014;**144**:19–25.
34. Reale L, Bonfigli F, Lai A *et al*. Contact X-ray microscopy of living cells by using LiF crystal as imaging detector. *J Microsc* 2015;**258**:127–39.
35. Villa MM, Wang L, Huang J *et al*. Bone tissue engineering with a collagen-hydroxyapatite scaffold and culture expanded bone marrow stromal cells. *J Biomed Mater Res B* 2015;**103**:243–53.

36. Caneva M, Botticelli D, Morelli F *et al*. Alveolar process preservation at implants installed immediately into extraction sockets using deproteinized bovine bone mineral – an experimental study in dogs. *Clin Oral Implants Res* 2012;**23**:789–96.
37. Bhuiyan D, Jablonsky MJ, Kolesov I *et al*. Novel synthesis and characterization of a collagen-based biopolymer initiated by hydroxyapatite nanoparticles. *Acta Biomater* 2015;**15**:181–90.
38. Winter W, Krafft T, Steinmann P *et al*. Quality of alveolar bone – Structure-dependent material properties and design of a novel measurement technique. *J Mech Behav Biomed Mater* 2011;**4**:541–8.
39. Yachouh J, Domergue S, Hoarau R *et al*. Biomechanics of the weakened mandible: use of image correlation analysis. *Br J Oral Maxillofac Surg* 2013;**51**:e137–41.
40. TenHuisen KS, Martin RI, Klimkiewicz M *et al*. Formation and properties of a synthetic bone composite: hydroxyapatite-collagen. *J Biomed Mater Res* 1995;**29**:803–10.
41. Chao KH, Lai YS, Chen WC *et al*. Biomechanical analysis of different types of pedicle screw augmentation: a cadaveric and synthetic bone sample study of instrumented vertebral specimens. *Med Eng Phys* 2013;**35**:1506–12.